Journal of The Electrochemical Society, **157** (7) A808-A811 (2010)
0013-4651/2010/157(7)/A808/4/$28.00 © The Electrochemical Society

Electrochemical Performance of $LiMnPO_4$ Synthesized with Off-Stoichiometry

Byoungwoo Kang and Gerbrand Ceder[*,z]

Department of Materials Science and Engineering, Massachusetts Institute of Technology, Cambridge, Massachusetts 02139, USA

$LiMnPO_4$ was synthesized from an off-stoichiometric mix of starting materials with nominal composition $LiMn_{0.9}P_{0.95}O_{4-\delta}$. Stoichiometric $LiMnPO_4$ with particle size <50 nm was found with X-ray diffraction even with the large overall deviation from stoichiometry in the sample, indicating that other noncrystalline compounds are present. The off-stoichiometric sample had a discharge capacity of 145 mAh/g at C/10 and ~100 mAh/g at 2C after a constant current constant voltage charge. Capacity retention was excellent without a significant capacity loss at 1C. The performance of $LiMn_{0.9}P_{0.95}O_{4-\delta}$ could not be significantly improved by diluting the electrode with more carbon, indicating a more intrinsic kinetic limitation of the material for $LiMnPO_4$ in contrast to $LiFePO_4$ [*Nature (London)*, **458**, 190 (2009)]. This is further corroborated by the difference in the overpotential between the two materials. Although $LiMnPO_4$ has a sloping voltage profile, $LiFePO_4$ tends to have a constant overpotential at high rate.
 [DOI: 10.1149/1.3428454]

Manuscript submitted December 15, 2009; revised manuscript received March 22, 2010. Published May 14, 2010.

The family of $LiMPO_4$ compounds is of interest as cathode materials for rechargeable lithium batteries. $LiFePO_4$ has been intensely studied and several techniques such as carbon coating, coating with a metallic conducting layer,[1] and doping with supervalent elements[2] have been shown to enhance the performance of $LiFePO_4$. Also, reducing the particle size is particularly effective for improving performance.[3,4] Although $LiMnPO_4$ shows a higher potential[5-7] than $LiFePO_4$, the higher energy density of $LiMnPO_4$ can only be achieved at a very slow rate.[5,6] Previous studies suggested several possible culprits for the poor activity: strong polarons,[6] very poor electronic conductivity (2.7×10^{-9} S cm^{-1} at 300°C),[5] the instability of $MnPO_4$,[8] the distortion of the Jahn–Teller active Mn^{3+} ion,[9] the large volumetric change between $LiMnPO_4$ and $MnPO_4$ during charge/discharge,[10] or the high activation barrier for Li to cross the surface.[11] Good electrochemical performance was recently observed for thin platelike carbon-coated $LiMnPO_4$ with a small particle size synthesized by a polyol process[12,13] or a sol–gel process.[14] In this paper, we report on an alternative way to create small particles of $LiMnPO_4$ with reasonable performance. The approach is similar to our recently developed approach to synthesize small $LiFePO_4$ particles through a simple solid-state reaction by starting with the proper off-stoichiometry of precursors.[15] As this off-stoichiometric $LiFePO_4$ showed excellent rate performance, we applied the same strategy to $LiMnPO_4$.

Experimental

The materials with the nominal formula $LiMn_{0.9}P_{0.95}O_{4-\delta}$ were synthesized from the appropriate mix of Li_2CO_3, $MnC_2O_4 \cdot 2H_2O$, and $NH_4H_2PO_4$ using heat-treatments at 350°C for 10 h and at 700°C for 10 h under Ar or air atmosphere. Before heat-treatment at 350°C, the precursors were ballmilled in acetone with zirconia balls. The structure and morphology was characterized by X-ray diffraction (XRD) and scanning electron microscopy (SEM). The X-ray patterns were obtained on a Rigaku diffractometer using Cu Kα radiation. The lattice parameters were determined by Rietveld refinement using the X'pert High Score Plus software. SEM was performed on an FEI Philips XL30 Field Emission Gun (FEG) Environmental Scanning Electron Microscopy (ESEM). The samples on the stainless holder were coated with gold/palladium to avoid charging effects.

Electrodes were prepared by manually mixing the active material, carbon (Super P from M.M.M.), and the binder (polyethylene-tetrafluoride) in a weight ratio of 80, 15, and 5%, respectively. The cells were assembled in an argon-filled glove box and tested on a Maccor 2200 operating in the galvanostatic mode using lithium metal as an anode, nonaqueous electrolyte [1 M $LiPF_6$ in ethyl carbonate:dimethyl carbonate (1:1) from Merck], and Celgard 2500 as a separator in a Swagelok-type cell. All cells were tested at room temperature. The loading density of electrodes was 3–5 mg/cm^2. The current density at 1C was based on a capacity of 170 mAh/g. All cell tests had 1 min open-circuit rest at the end of each charge and discharge.

Results and Discussion

Characterization of the off-stoichiometric $LiMnPO_4$.— Figure 1 shows the XRD pattern of $LiMnPO_4$ and $LiMn_{0.9}P_{0.95}O_{4-\delta}$ synthesized at 700°C under Ar. The pattern in Fig. 1b indicates the formation of $LiMnPO_4$ despite the large off-stoichiometry in the starting materials. This result is similar to what is observed when off-stoichiometric $LiFePO_4$ [15] is prepared. Rietveld refinement using $LiMnPO_4$ as the structural model gives lattice parameters of $a = 10.4366(4)$ Å, $b = 6.0994(2)$ Å, and $c = 4.7430(2)$ Å for the off-stoichiometric sample and $a = 10.4367(5)$ Å, $b = 6.0991(3)$ Å, and $c = 4.7436(2)$ Å for the stoichiometric sample. These values are consistent with previously reported values,[8] confirming that the crystalline phase in the off-stoichiometric sample is close to stoichiometric $LiMnPO_4$.

The crystallite size obtained from the XRD pattern is ~340 Å for the off-stoichiometric sample and ~337 Å for the stoichio-

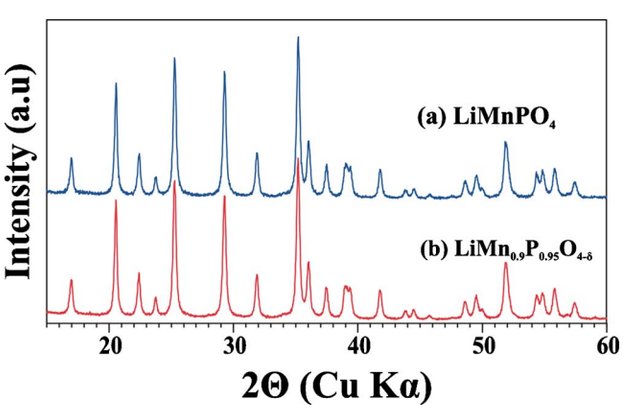

Figure 1. (Color online) XRD patterns of (a) $LiMnPO_4$ and (b) $LiMn_{0.9}P_{0.95}O_{4-\delta}$ synthesized at 700°C under Ar.

* Electrochemical Society Active Member.
z E-mail: gceder@mit.edu

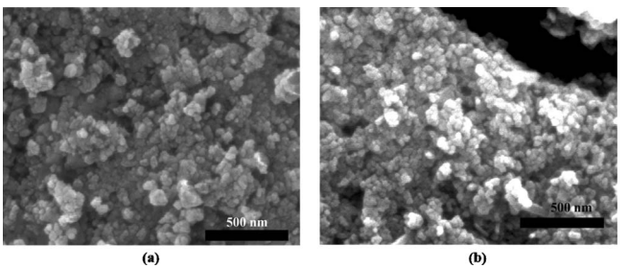

Figure 2. SEM images of (a) $LiMnPO_4$ and (b) $LiMn_{0.9}P_{0.95}O_{4-\delta}$ synthesized at 700°C under Ar.

metric sample. The SEM images in Fig. 2 show a spherelike morphology and particle size less than 50 nm for both samples.

Analysis of the secondary-phase components.— Considering the significant deviation from the stoichiometric composition, the off-stoichiometric sample should have secondary phases present as $LiMPO_4$ cannot accommodate such a large compositional deviation. For $LiFePO_4$, Wagemaker et al.[16] and Meethong et al.[17] reported that a single phase could only be retained for less than 5 mol % deviation from stoichiometry in the overall sample.

Assuming that a near stoichiometric $LiMnPO_4$ is formed in the off-stoichiometric sample, the balance of products should be phases containing Li–P–O. According to the Li–Mn–P–O phase diagram obtained through first-principles calculations, the off-stoichiometric material forms either $Li_4P_2O_7$, Li_3PO_4, $LiMnP_2O_7$, or a combination of these as secondary phases depending on the oxidation conditions and the range of composition in which these phases exist.[18] Although the first-principles calculations assume stoichiometric compounds, it is possible that these secondary phases are not stoichiometric, particularly given their amorphous or poorly crystallized nature. We indeed see some of these secondary phases when the material is fired at 700°C under air. Figure 3 indicates that crystalline Li_3PO_4 and $Li_4P_2O_7$ appear in the XRD pattern, whereas the $LiMnPO_4$ phase is unchanged. Rietveld refinement of the air-synthesized off-stoichiometric sample gives the weight percentage of $LiMnPO_4$ as 95 wt %.

The amorphous nature of the secondary phases when synthesis is performed under Ar can be understood by the fact that phosphorus, like silicon or boron in glasses, acts as a network former.[19] Alkali, earth alkali, or transition-metal oxides act as network modifiers in silicon, boron, and phosphate glasses. Therefore, the phosphate network in the glasses is likely to depend on manganese oxide contents. As the manganese oxide content increases, the phosphate network changes from a chain or ring structure, such as in metaphosphates (PO_3^-), through the diametric pyrophosphate ($P_2O_7^{4-}$), to the isolated orthophosphate (PO_4^{3-}).[20,21] Hence, a high Mn to P ratio such as in

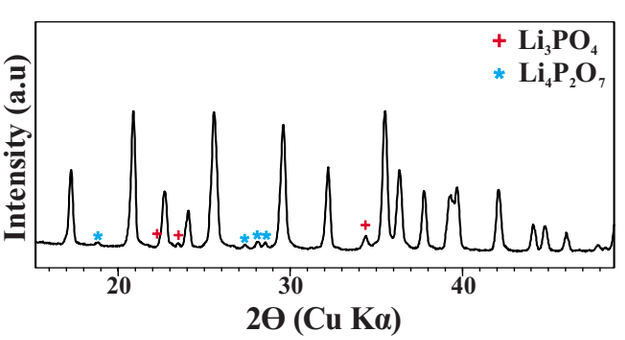

Figure 3. (Color online) XRD pattern of $LiMn_{0.9}P_{0.95}O_{4-\delta}$ synthesized at 700°C under air. $LiMnPO_4$, Li_3PO_4, and $Li_4P_2O_7$ are present.

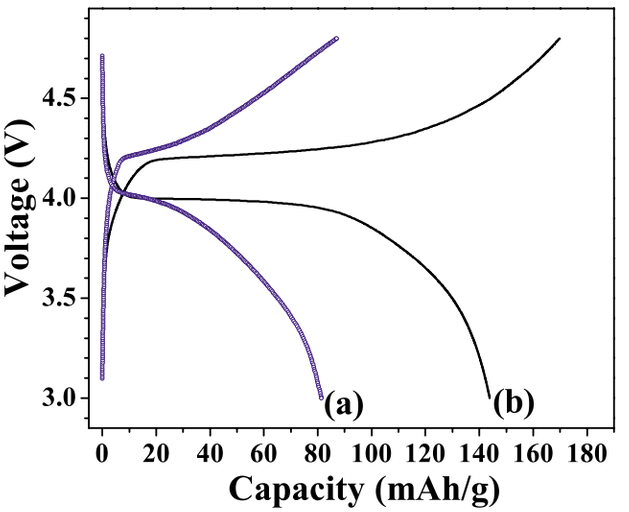

Figure 4. (Color online) (a) Voltage profiles of $LiMnPO_4$ at C/20 and (b) $LiMn_{0.9}P_{0.95}O_{4-\delta}$ at C/20.

$LiMnPO_4$ leads to a crystalline compound, whereas under the same conditions, the secondary phase with a low Mn to P ratio may be noncrystalline. The crystallinity of these phases also depends on synthesis conditions[21,22] such as temperature and atmosphere.

The poorly crystallized phase induced by the off-stoichiometry is likely to be responsible for the small particle size. As stoichiometric $LiMnPO_4$ forms, it rejects the balance of composition into a secondary phase, which sits at the surface and between the grains of $LiMnPO_4$. A similar observation was made in off-stoichiometric $LiFePO_4$.[23] Possibly, this secondary phase prevents grain growth by limiting the diffusion between particles or grains similar to the role of carbon in carbon-coated $LiFePO_4$ compound[24-26] or by reducing the surface energy of the material.[27]

Electrochemical performance.— The theoretical capacity of stoichiometric $LiMnPO_4$ is 171 mAh/g. The theoretical capacity of the off-stoichiometric sample is more difficult to assess. If we assume that the $LiMn_{0.9}P_{0.95}O_{4-\delta}$ sample consists of $LiMnPO_4$ and a phase with composition $Li_4P_2O_7$, the theoretical capacity would be 166 mAh/g. Using, however, the refined phase fractions from the sample synthesized at 700°C in air, the theoretical capacity would be 162 mAh/g, assuming that only the $LiMnPO_4$ fraction is active. The voltage profiles of the stoichiometric and the off-stoichiometric samples at C/20 are shown in Fig. 4. The off-stoichiometric sample (Fig. 4b) shows a flat potential around 4.15 V vs Li/Li^+, which is the typical redox potential of Mn^{2+}/Mn^{3+} in the olivine structure[5,28] and achieves 145 mAh/g (87–89% of theoretical capacity) in the constant current mode for both charge and discharge. However, the stoichiometric sample in Fig. 4a shows a sloping voltage profile with only ~80 mAh/g capacity at the same rate.

Figure 5 shows the capacity retention of the off-stoichiometric and stoichiometric samples at 1C rate. Both materials show good capacity retention with cycling. The off-stoichiometric sample achieves 65 mAh/g at 1C, about twice the capacity of $LiMnPO_4$. The capacity of the off-stoichiometric sample at 1C is similar to that of the stoichiometric sample at C/20, indicating a remarkable improvement of rate capability by creating $LiMnPO_4$ in an off-stoichiometric sample.

Rate Capability

Figure 6 shows the rate capability of $LiMn_{0.9}P_{0.95}O_{4-\delta}$ in an electrode with 15 wt % carbon. The cell was charged at C/20 and held at 4.8 V until the current reached C/100. A discharge capacity of ~145 mAh/g is obtained at C/10 and ~100 mAh/g at 2C. The

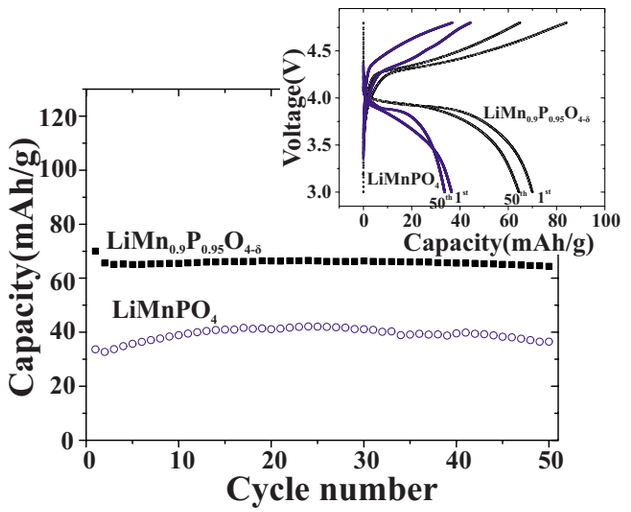

Figure 5. (Color online) Comparison of the capacity retention of $LiMn_{0.9}P_{0.95}O_{4-\delta}$ and $LiMnPO_4$ at 1C rate. The cell was charged at 1C and discharged at 1C in a voltage window from 3.0 to 4.8 V. The formulation of the electrode was 80:15:5 in a ratio of active, carbon, and binder in wt %, respectively. Inset shows the corresponding voltage profiles of $LiMn_{0.9}P_{0.95}O_{4-\delta}$ and $LiMnPO_4$ at 1st and 50th cycles at 1C rate.

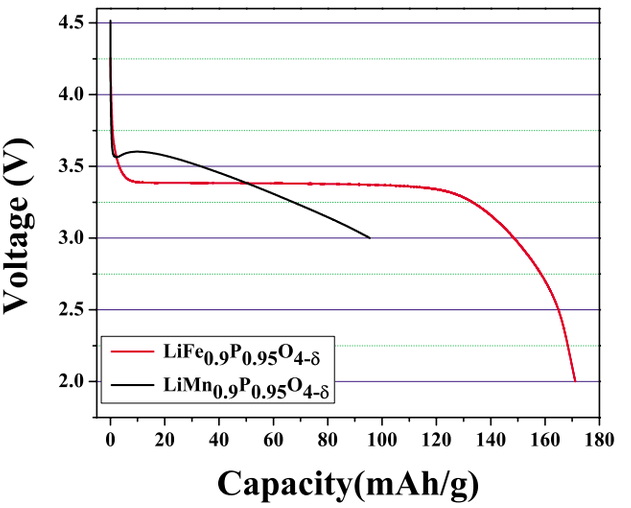

Figure 7. (Color online) Comparison of the discharge behavior of $LiMn_{0.9}P_{0.95}O_{4-\delta}$ and $LiFe_{0.9}P_{0.95}O_{4-\delta}$. Both materials were discharged at 2C. The $LiMnPO_4$ data are the same as in Fig. 6. The off-stoichiometric $LiFePO_4$ was charged at C/5 and held at 4.3 V until the current reached C/20.

voltage dip at the beginning of discharge at 2C may be related to the nucleation[29] of the $LiMnPO_4$ phase but actually leads to less polarization than the 1C voltage profile at the end of discharge. Also, somewhat surprisingly, the capacity at 2C is larger than that at 1C in Fig. 6. The difference may be related to the nucleation behavior. The larger rate at 2C drives the material toward larger underpotential, which causes a higher nucleation rate in the particles. This may ultimately lead to larger accessible capacity. Unlike what is observed in $LiFePO_4$,[5,15] the voltage profiles at all rates are sloping in Fig. 6. In contrast to the data in Fig. 4 the curves in Fig. 6 are obtained after a constant current and constant voltage (CCCV) charge.

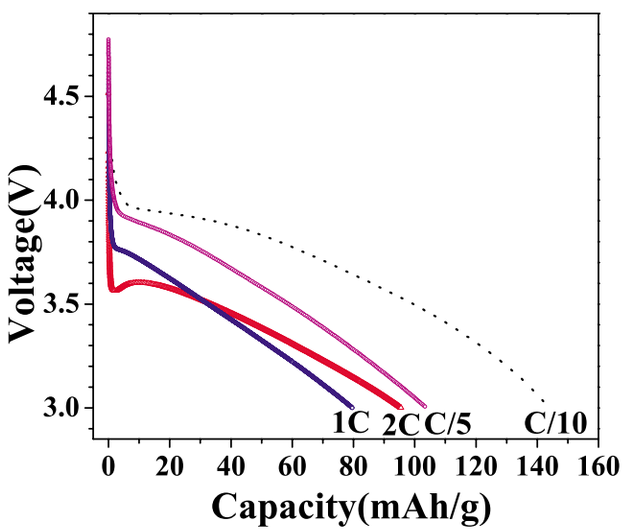

Figure 6. (Color online) Rate capability of $LiMn_{0.9}P_{0.95}O_{4-\delta}$ synthesized at 700°C under Ar. The cell was charged at C/20 and held at 4.8 V until the current reached C/100, and then discharged at various rates. The discharge test at 2C was the first cycle. The sequence of the discharge tests: 2C → C/10 → 1C → C/5. The voltage window is 3.0–4.8 V.

The discharge profile of $LiFe_{0.9}P_{0.95}O_{4-\delta}$ [15] and $LiMn_{0.9}P_{0.95}O_{4-\delta}$ at 2C are compared in Fig. 7. Although $LiFe_{0.9}P_{0.95}O_{4-\delta}$ shows a flat discharge profile ~3.4 V, $LiMn_{0.9}P_{0.95}O_{4-\delta}$ shows a clear nucleation barrier and a sloping voltage profile, indicating that the two materials may have fundamentally different transformation kinetics.

To test if the electrode preparation controls the high rate performance (as was the case for $LiFePO_4$ [15]), we also tested electrodes with 65 wt % carbon. Even at this high dilution of active material in the electrode, only 140 mAh/g is obtained at C/10 and 70 mAh/g at 3C as shown in Fig. 8. These capacities are quite similar to the capacities obtained for the electrode with 15 wt % C in Fig. 4, indicating that the rate performance of $LiMn_{0.9}P_{0.95}O_{4-\delta}$ is limited by the active material rather than by the transport through the composite electrode, as is the case for high rate $LiFePO_4$.[15,30] Although not much capacity is obtained by increasing the electrode's carbon content, there is a lowering of the polarization compared to the low carbon electrode.

Discussion

$LiMnPO_4$ shows a rather limited electrochemical activity even with a small particle size obtained by a variety of processes.[6,31] Even at a very low rate such as C/100 or C/20, the capacity is well below the theoretical capacity. As in $LiFePO_4$, creating a Mn/P 2:1 deficiency improves the rate capability, obtaining up to 100 mAh/g at 2C. Although the small particle size likely contributes to the enhanced rate capability, it is not the only factor as materials with comparable particle size[6,12] and the stoichiometric samples achieve less capacity at 1C than $LiMnPO_4$ created in our off-stoichiometric sample.

The improvement of the rate capability using off-stoichiometry was not as substantial for $LiMnPO_4$ as that observed in $LiFe_{0.9}P_{0.95}O_{4-\delta}$. This result could point at fundamentally different kinetics of the two compounds. Unfortunately, no precise model exists for the kinetics of phase transformation in $LiFePO_4$ or $LiMnPO_4$. The voltage profiles of $LiFePO_4$ and $LiMnPO_4$ also point at a substantial difference between the two materials. The $LiFePO_4$ compound shows a flat potential, whereas a sloping voltage[12,32] is observed in $LiMnPO_4$. The sloping voltage profile can arise from several factors. Gaberscek et al.[30] claims that the sloping voltage arises from transport limitations in the electrode, not from the material. However, formulating the electrode with 65 wt % carbon (Fig. 8) to facilitate electron transfer did not lead to any significant im-

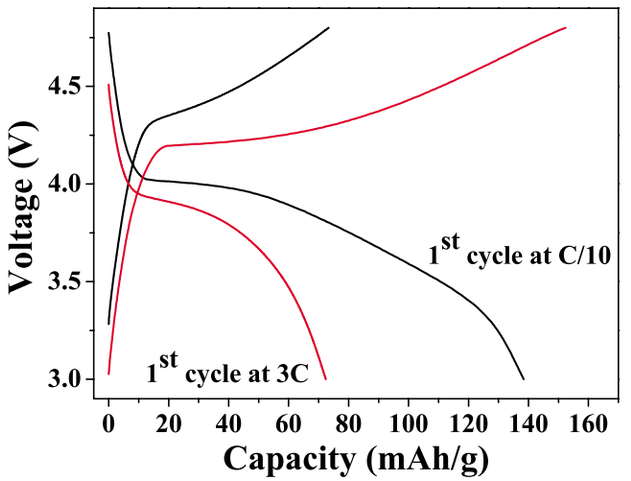

Figure 8. (Color online) Electrochemical performance of the electrode formulated with 65 wt % carbon in $LiMn_{0.9}P_{0.95}O_{4-\delta}$. The cells were charged and discharged in constant current mode. The loading density of the electrode with 65 wt % carbon was 3.61 mg/cm. The voltage window is 3.0–4.8 V.

provement in the electrochemical performance compared to 15 wt % carbon. Therefore, the performance of $LiMnPO_4$ depends considerably less on the formulation of the electrode than for off-stoichiometric $LiFePO_4$.[15] Instead, we speculate that the sloping voltage profile may be related to nucleation problems. The constant current testing condition imposes a constant phase transformation rate of $MnPO_4$ to $LiMnPO_4$ in a galvanostatic discharge. The rate at which nuclei form is the nucleation rate (I) per unit volume times the volume (V) of the untransformed phase. As discharge proceeds, the volume of the untransformed material decreases and the nucleation rate (I) has to increase to keep the applied current constant. A larger underpotential is required to generate a higher nucleation rate as the discharge proceeds, leading to a sloping voltage curve. The absence of the slope in the discharge of a well-optimized $LiFePO_4$ electrode may indicate that nucleation is less important for $LiFePO_4$.

Conclusion

We synthesized $LiMnPO_4$ with small particles using the proper off-stoichiometry to create a poorly crystallized second phase. $LiMnPO_4$ synthesized from an off-stoichiometric mixture has improved electrochemical performance over stoichiometric samples: 145 mAh/g discharge capacity at C/10 and ~100 mAh/g at 2C after a CCCV charge mode. The capacity retention at 1C charge/discharge was excellent without degradation of the capacity for 50 cycles. Unlike $LiFe_{0.9}P_{0.95}O_{4-\delta}$, the $LiMnPO_4$ compound shows less benefits in rate capability from reducing its loading density in the electrode by increasing the carbon content, indicating that the material itself is rate-limiting. This evidence, together with the different shape of the overpotential between $LiFePO_4$ and $LiMnPO_4$, points at fundamentally different transformation kinetics in the two materials.

Acknowledgment

This work was supported by the BATT program under contract no. DE-AC02-05CH1123 (subcontract no. PO6806960) and by the U.S. National Science Foundation through the Materials Research Science and Engineering Centers program under contract no. DMR-0819762.

Massachusetts Institute of Technology assisted in meeting the publication costs of this article.

References

1. P. S. Herle, B. Ellis, N. Coombs, and L. F. Nazar, *Nature Mater.*, **3**, 147 (2004).
2. S. Y. Chung, J. T. Bloking, and Y. M. Chiang, *Nat. Mater.*, **1**, 123 (2002).
3. C. Delacourt, P. Poizot, S. Levasseur, and C. Masquelier, *Electrochem. Solid-State Lett.*, **9**, A352 (2006).
4. D. H. Kim and J. Kim, *Electrochem. Solid-State Lett.*, **9**, A439 (2006).
5. C. Delacourt, L. Laffont, R. Bouchet, C. Wurm, J. B. Leriche, M. Morcrette, J. M. Tarascon, and C. Masquelier, *J. Electrochem. Soc.*, **152**, A913 (2005).
6. M. Yonemura, A. Yamada, Y. Takei, N. Sonoyama, and R. Kanno, *J. Electrochem. Soc.*, **151**, A1352 (2004).
7. F. Zhou, M. Cococcioni, K. Kang, and G. Ceder, *Electrochem. Commun.*, **6**, 1144 (2004).
8. G. Y. Chen, J. D. Wilcox, and T. J. Richardson, *Electrochem. Solid-State Lett.*, **11**, A190 (2008).
9. A. Yamada, M. Yonemura, Y. Takei, N. Sonoyama, and R. Kanno, *Electrochem. Solid-State Lett.*, **8**, A55 (2005).
10. N. Meethong, H. Y. S. Huang, S. A. Speakman, W. C. Carter, and Y. M. Chiang, *Adv. Funct. Mater.*, **17**, 1115 (2007).
11. L. Wang, F. Zhou, and G. Ceder, *Electrochem. Solid-State Lett.*, **11**, A94 (2008).
12. T. R. Kim, D. H. Kim, H. W. Ryu, J. H. Moon, J. H. Lee, S. Boo, and J. Kim, *J. Phys. Chem. Solids*, **68**, 1203 (2007).
13. D. Y. Wang, H. Buqa, M. Crouzet, G. Deghenghi, T. Drezen, I. Exnar, N. H. Kwon, J. H. Miners, L. Poletto, and M. Graetzel, *J. Power Sources*, **189**, 624 (2009).
14. T. Drezen, N. H. Kwon, P. Bowen, I. Teerlinck, M. Isono, and I. Exnar, *J. Power Sources*, **174**, 949 (2007).
15. B. Kang and G. Ceder, *Nature (London)*, **458**, 190 (2009).
16. M. Wagemaker, B. L. Ellis, D. Luetzenkirchen-Hecht, F. M. Mulder, and L. F. Nazar, *Chem. Mater.*, **20**, 6313 (2008).
17. N. Meethong, Y. H. Kao, S. A. Speakman, and Y. M. Chiang, *Adv. Funct. Mater.*, **19**, 1060 (2009).
18. S. P. Ong, A. Jain, G. Hautier, B. Kang, and G. Ceder, *Electrochem. Commun.*, **12**, 427 (2010).
19. P. W. McMillan, *Glass-Ceramics*, Academic Press, London (1979).
20. A. Mogus-Milankovic, M. Rajic, A. Drasner, R. Trojko, and D. E. Day, *Phys. Chem. Glasses*, **39**, 70 (1998).
21. A. Mogus-Milankovic, B. Pivac, K. Furic, and D. E. Day, *Phys. Chem. Glasses*, **38**, 74 (1997).
22. A. Karthikeyan, P. Vinatier, A. Levasseur, and K. J. Rao, *J. Phys. Chem. B*, **103**, 6185 (1999).
23. A. Kayyar, H. J. Qian, and J. Luo, *Appl. Phys. Lett.*, **95**, 221905 (2009).
24. G. Kobayashi, S. I. Nishimura, M. S. Park, R. Kanno, M. Yashima, T. Ida, and A. Yamada, *Adv. Funct. Mater.*, **19**, 395 (2009).
25. Z. H. Chen and J. R. Dahn, *J. Electrochem. Soc.*, **149**, A1184 (2002).
26. P. P. Prosini, D. Zane, and M. Pasquali, *Electrochim. Acta*, **46**, 3517 (2001).
27. M. W. Barsoum, *Fundamentals of Ceramics*, p. 302, Institute of Physics, Bristol (2003).
28. G. H. Li, H. Azuma, and M. Tohda, *Electrochem. Solid-State Lett.*, **5**, A135 (2002).
29. K. E. Thomas, J. Newman, and R. M. Darling, in *Advances in Lithium-Ion Batteries*, W. A. van Schalkwijk and B. Scrosati, Editors, p. 363, Kluwer Academic Publishers, New York (2002).
30. M. Gaberscek, R. Dominko, and J. Jamnik, *Electrochem. Commun.*, **9**, 2778 (2007).
31. C. Delacourt, P. Poizot, M. Morcrette, J. Tarascon, and C. Masquelier, *Chem. Mater.*, **16**, 93 (2004).
32. A. Vadivel Murugan, T. Muraliganth, and A. Manthiram, *J. Electrochem. Soc.*, **156**, A79 (2009).